Ground vibration testing and fem model updating of scaled Diana 2 glider model using accelerometer, gyro and strain measurements

Jürisson, Andres; Timmermans, Huub; Eussen, Bart; de Visser, Coen; de Breuker, Roeland

Publication date
2022

Document Version
Final published version

Published in
Proceedings of the International Forum of Aeroelasticity and Structural Dynamics 2022, IFASD 2022

International Forum on Aeroelasticity and Structural Dynamics
IFASD 2022
13-17 June 2022, Madrid, Spain

GROUND VIBRATION TESTING AND FEM MODEL UPDATING OF SCALED DIANA 2 GLIDER MODEL USING ACCELEROMETER, GYRO AND STRAIN MEASUREMENTS

Andres Jürisson[1,2], Huub Timmermans[1], Bart Eussen[1], Coen de Visser[2], Roeland de Breuker[2]

[1]Netherlands Aerospace Centre
Anthony Fokkerweg 2, 1059 CM, Amsterdam, The Netherlands
Andres.Jurisson@nlr.nl
Huub.Timmermans@nlr.nl
Bart.Eussen@nlr.nl

[2]Delft University of Technology
Kluyverweg 1, 2629 HS Delft, The Netherlands
c.c.devisser@tudelft.nl
R.DeBreuker@tudelft.nl

Keywords: ground vibration testing, gyroscopes, strain gauges, experimental modal analysis, strain modal analysis, FEM updating, IMUs

Abstract: A ground vibration test was conducted with a 1:3 scaled Diana 2 glider model where the modal parameters were estimated using the accelerometers, gyroscopes and strain gauges integrated in the test aircraft and validated using externally attached calibrated accelerometers and commercial software. These modal parameters were then used to update a FEM model of the glider together with static load tests and component mass measurements. The goal for this updated and fitted FEM model is then to build an aeroelastic model for flexible aircraft flight dynamics simulator.

1 INTRODUCTION

To be able to investigate system identification of flexible aircraft, Netherlands Aerospace Centre (NLR) acquired a 1:3 scaled Diana 2 glider model to serve as an aeroelastic flight testing platform. The glider was instrumented with numerous sensors to capture the response of the aircraft flight dynamics together with its structural dynamics. These included accelerometers, gyroscopes and strain gauges placed across the aircraft structure as part of an in-house and custom built data acquisition (DAQ) system [1].

As the glider model was not built in house and a custom solution for the DAQ was used, it was necessary to characterise its structural properties in an experimental manner while also evaluating the accuracy of the integrated sensors at capturing the modal parameters. Furthermore, a FEM model was required to build an aeroelastic flight dynamics simulator to explore different system identification approaches and compare the identified models. Therefore, a ground vibration test campaign was performed to achieve these goals.

In this paper, a ground vibration test of the scaled Diana 2 glider is performed using the internal accelerometers, gyroscopes and strain gauges. The modal parameter estimates are then compared to results obtained using externally attached calibrated accelerometers. Using the GVT results together with component mass and stiffness measurements, a FEM model of the aircraft is updated. The accuracy of the structural model is then determined by comparing the model outputs with a ground vibration test where lumped mass modifications were added to the glider.

2 THEORETICAL BACKGROUND

During the ground vibration testing, the aircraft structure is excited and the responses together with the excitation force are collected. These measurements are then used to perform an experimental modal analysis with the goal of estimating the modal parameters of the structure. These parameters consist of natural frequencies, damping and mode shapes which can be used to characterise the behaviour of the structure. Using the modal parameters, the steady state response of the structure can be represented in the frequency domain as [2]:

$$\mathbf{X}(\omega) = \mathbf{\Phi}[\omega_n^2 - \omega^2 + i2\omega_n\zeta\omega]^{-1}\mathbf{\Phi}^T\mathbf{F}(\omega) = \mathbf{H}(\omega)\mathbf{F}(\omega) \tag{1}$$

where $\mathbf{X}(\omega)$ and $\mathbf{F}(\omega)$ contain the degrees of freedom and the applied force. While ω is the circular frequency and $\mathbf{\Phi}$, ω_n and ζ_n are the mode shape matrix, nth natural frequency and damping respectively. From the test measurements, the frequency response functions (FRFs) are calculated that contain the parameters of interest and make up the FRF matrix $\mathbf{H}(\omega)$.

$$\mathbf{H}(\omega) = \sum_{n=1}^{N} \frac{\mathbf{\Phi}_n\mathbf{\Phi}_n^T}{\omega_n^2 - \omega^2 + i2\omega_n\zeta\omega} \tag{2}$$

In the conventional modal testing, the displacement, velocity or acceleration measurements are collected. However, in the case where rotational rate responses are measured instead, a similar derivation approach can be used. Now in place of the translational degrees of freedom contained in $\mathbf{X}(\omega)$ are the rotational degrees of freedom.

A third option would be to measure the strain responses of the structure. In order to transform from displacements to strains an operator $\mathbf{S}$ is introduced where $\triangledown$ is the linear differential operator [2]. This allows to represent the strain mode shape $\mathbf{\Psi}_n$ corresponding to the n-th displacement mode shape $\mathbf{\Phi}_n$.

$$\mathbf{S} = \frac{1}{2}(\triangledown + \triangledown^T) \tag{3}$$

$$\mathbf{\Psi}_n = \mathbf{S}\mathbf{\Phi}_n \tag{4}$$

From the test measurements then the strain FRF matrix $\mathbf{H}^\varepsilon(\omega)$ is determined instead.

$$\mathbf{H}^\varepsilon(\omega) = \sum_{n=1}^{N} \frac{\mathbf{\Psi}_n\mathbf{\Phi}_n^T}{\omega_n^2 - \omega^2 + i2\omega_n\zeta\omega} \tag{5}$$

With the determined mode shapes it is then possible to approximate the response of the structure as a summation of N modes.

$$X(t) \approx \sum_{n=1}^{N} \Phi_n\eta_n(t) = \boldsymbol{\Phi\eta} \tag{6}$$

where $\eta_n(t)$ is the modal amplitude.

3 EXPERIMENTAL SETUP

3.1 Diana 2 scaled glider overview

The ground vibration testing was conducted on a 1:3 scaled Diana 2 glider manufactured by Baudismodel [3]. This composite glider model has a wingspan of 5 m at an aspect ratio of 24.3. An overview of the main technical parameters of the model are presented in Table 1 together with a picture of the glider shown in Figure 1.

Table 1: Diana 2 model technical data.

Property	Symbol	Value
Aspect ratio	Λ	24.3
Wingspan	b	5.0 m
Wing area	S	1.03 m^2
Mean chord	$\bar{c}$	0.206 m
Weight	m	11.25 kg

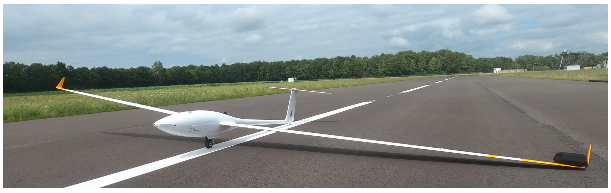

Figure 1: Diana 2 1:3 scaled glider.

The model was instrumented with ICM-20948 MEMS inertial measurement units (IMU), strain gauges and other sensors as presented in [1]. An overview of these sensors and their placement is presented in Figure 2.

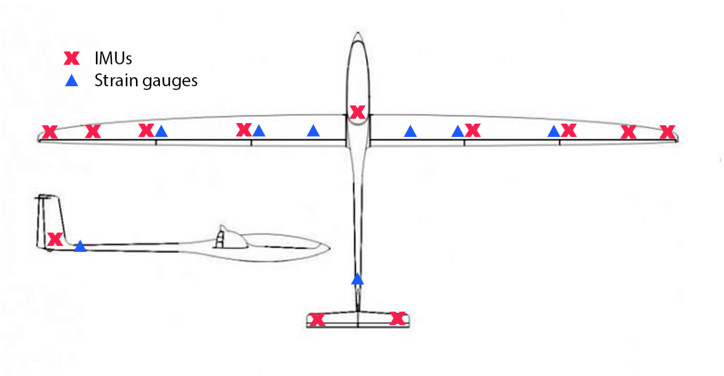

Figure 2: Diana 2 integrated sensor placement overview.

At each IMU location, the acceleration and rotational rates are measured in all three directions. At each strain gauge location on the wings, there is one strain gauge in full bridge configuration for bending (EA-06-250PD-350) and two for shear (CEA-06-250US-350). The strain gauges for shear are placed in front and behind the main spar as can be seen in Figure 3. At the tail, there is one strain gauge for shear to measure the torsion of the T-tail and two strain gauges for bending to measure the horizontal and vertical forces. The strain gauges are supplied with an excitation voltage of 5.1V while an ADS1115 analog to digital sensors are used to measure the strain gauge voltage outputs. In total, 36 acceleration and rotational rate and 21 strain responses are measured. The measurements are collected using a custom built data acquisition system based on a Raspberry Pi running open source Robot Operating System (ROS) software.

Figure 3: Strain gauge placement on the wings.

3.2 Ground vibration test setup

For the ground vibration test, the scaled glider model was suspended in the air with elastic bands and excited at multiple locations with an impulse hammer. This setup can be seen in Figure 4. The responses of the structure were then measured using the internal accelerometers, gyroscopes and strain gauges and in addition also a set of external accelerometers were used for reference. The external accelerometer locations and measurement directions are presented in Figure 5. They were placed to match the locations of the internal sensors together with some additional accelerometers used to capture the torsion of the wings. In total 5 triaxial (PCB 356A33) and 30 single axis (PCB 352C22) accelerometers were used. These external sensors were collected using a SCADAS system together with Siemens Testlab.

Figure 4: Ground vibration testing setup.

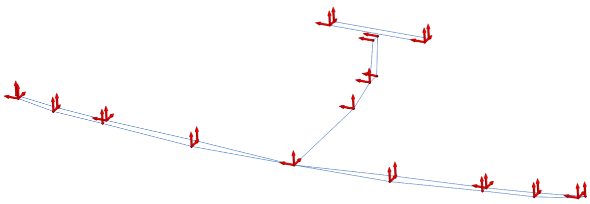

Figure 5: Reference accelerometer locations for GVT.

As the structural responses were collected using two different systems (internal and external), it was necessary to split the impulse hammer output and connect it to both systems. This also allowed to synchronise both systems by recording the time signals for a given test location and direction. From these time signals the peaks corresponding to the hammer hits can be found and a time shift between the two systems could be determined. Instead of the traditional 3-5 hits per test location, 7 hits were performed to achieve a better estimate of the time shift and to improve the averaged FRFs for the internal sensors.

The IMUs installed in the glider are MEMS type sensors which means that they also capture the gravitational acceleration and other low frequency signals that traditionally filtered out. For example, the hammer impacts at some locations would cause a very slow frequency rigid body oscillation that in turn would result in an acceleration measurement due to gyroscopic effects. To remove these effects, a high pass filter was applied to the acceleration and rotational rate measurements of the internal sensors before the calculation of the FRFs. After calculating the FRFs for the internal and external sensors, they were imported to Siemens Testlab where the modal identification procedure was carried out.

4 MODAL PARAMETER ESTIMATION

The modal parameter estimation was conducted using the PolyMAX method [4] in Siemens Testlab. The internal accelerometer, gyroscope and strain FRFs were used simultaneously during the estimation process and were then compared to the results obtained using the external accelerometers. In Table 2 the estimated modes and their frequencies are presented for the reference accelerometers and internal sensors. As can be seen, the estimated modal frequencies obtained using the internal sensors closely match the reference with most modes having less than 1% difference. Furthermore, a comparison between the displacement mode shapes obtained from the reference and internal accelerometers was made using the modal assurance criterion (MAC) [5]:

$$MAC(\Phi_r, \Phi_s) = \frac{\left|\Phi_r^T \Phi_s\right|^2}{(\Phi_r^T \Phi_r)(\Phi_s^T \Phi_s)} \tag{7}$$

where Φ_r and Φ_s are the mode shape vectors being compared. The closer the MAC value is to one, the more similar the mode shapes are. These results are also presented in Table 2. Again an excellent match was obtained which shows that the internal data acquisition system is able to accurately capture the modal parameters of the structure. Only in mode 7 there was a node at the right wing tip that did not match the out of plane movement and therefore resulting in a lower MAC value.

Table 2: Reference accelerometer and internal sensor modal parameter estimation comparison.

Mode	Ref. [Hz]	Internal [Hz]	Diff. [%]	$MAC_{disp}[\%]$
1	7.56	7.57	-0.15	98.7
2	9.96	9.98	-0.18	99.2
3	14.19	14.18	0.03	98.7
4	17.31	17.33	-0.11	99.5
5	20.12	20.09	0.18	93.5
6	21.43	21.22	1.00	97.9
7	23.89	23.50	1.69	83.6
8	26.08	26.01	0.25	91.9
9	39.83	39.57	0.65	96.5
10	45.04	45.15	-0.25	94.2
11	47.18	46.94	0.50	97.7
12	53.05	53.11	-0.12	90.7

In Figure 6 to Figure 11, the first mode shapes obtained from the internal sensors are presented. Here the displacement corresponds to the displacement mode shapes. The arrows correspond to the rotational mode shapes and point in the resultant vector direction. Finally, the colours correspond to the strain mode shapes.

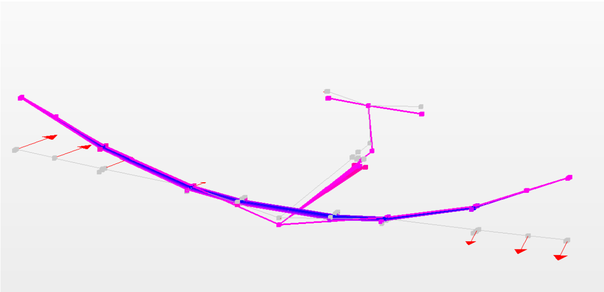

Figure 6: Mode 1 - 1st sym. wing bending.

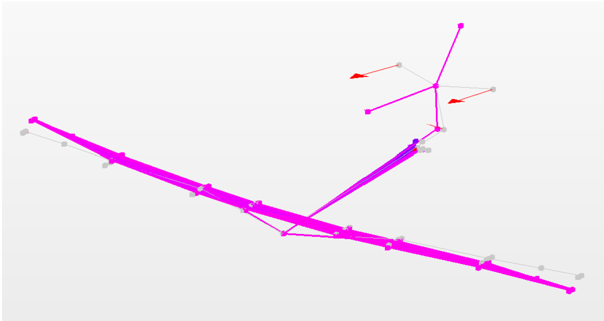

Figure 7: Mode 2 - tail rotation around x-axis.

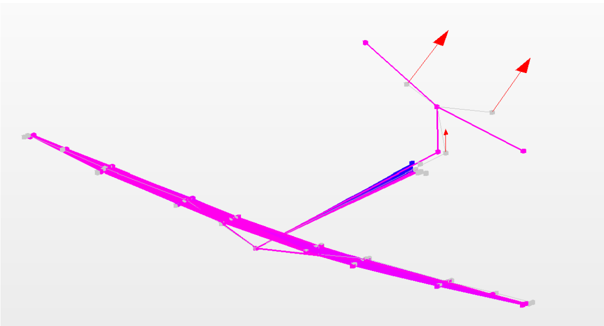

Figure 8: Mode 3 - tail rotation around z-axis.

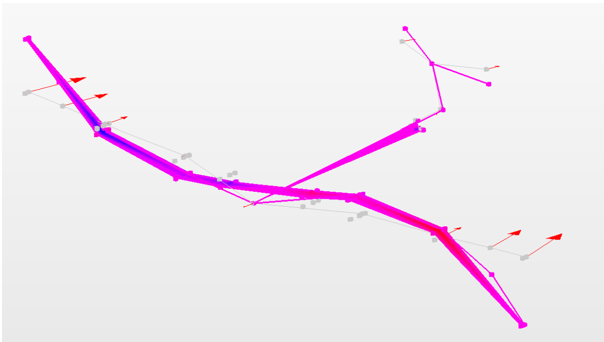

Figure 9: Mode 4 - 2nd asym. wing bending.

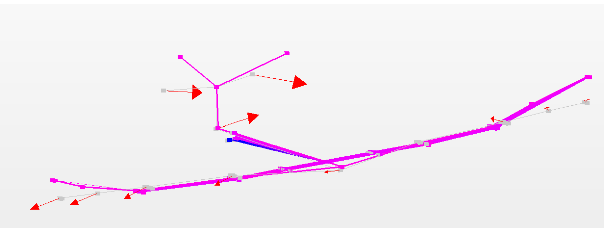

Figure 10: Mode 5 - horizontal tail 1st sym. bending.

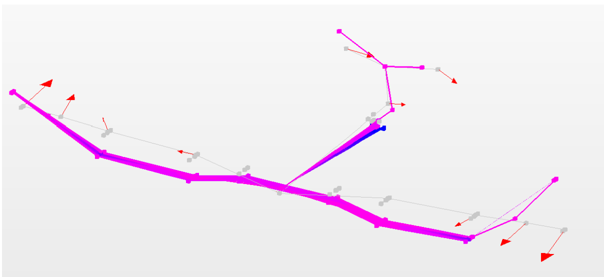

Figure 11: Mode 7 - 2nd sym. wing bending.

As was already shown in [6], using accelerometers and strain gauges simultaneously during the modal estimation, it is possible to obtain a better understanding and interpretation of the strain patterns and the corresponding displacement mode shapes. Now by adding also gyroscopes to the estimation, it is possible to directly measure the rotational mode shapes. This can give even more information about the structure or alternatively it would allow to remove the extra accelerometers used for capturing the torsion of the wings etc. Thereby reducing the number of locations that need to be instrumented for the GVT.

5 FEM MODEL UPDATING

An initial NASTRAN model was created for aeroelastic analysis based on the outer geometry of the Diana 2. However, as there was no information available about the structural properties, a simplified beam model was created. This allowed to evaluate different sensor placement options for the GVT. The outer geometry supplied by the manufacturer and the NASTRAN model are presented in Fig. 12.

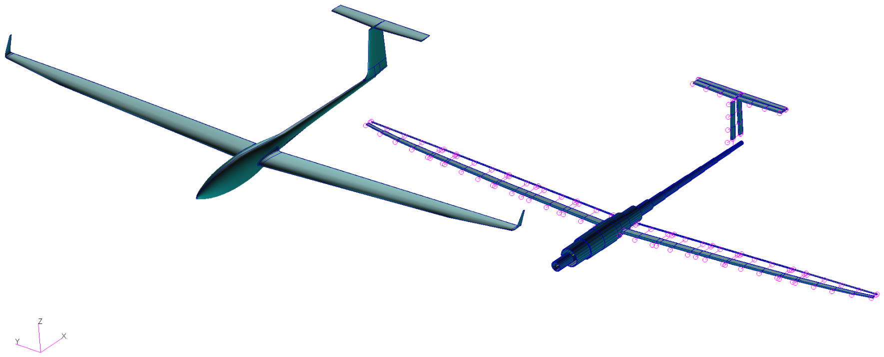

Figure 12: Diana 2 model outline and NASTRAN model.

Using the modal parameters obtained during the GVT, it was now possible to perform model updating based on the test results. In addition to the modal frequencies and mode shapes, also the mass and center of gravity of the wings and aircraft was measured which are presented in Table 3. The reference frame origin is at the nose of the aircraft with the x-axis pointing towards the tail and y-axis positive towards the right wing.

Table 3: Diana 2 weight and center of gravity measurements.

Element	Mass [kg]	CoG x [m]	CoG y [m]
Left wing	1.95		-0.975
Right wing	1.95		0.975
Fuselage	7.35		
Aircraft	11.25	0.74	0

Moreover, a load-displacement test was conducted on the wings to gather information about their stiffness properties. During the testing, first the wing tips were loaded and then additional load was applied 1m from the wing tips while measuring the displacement responses. The test results can be seen in Figure 13. The top figure shows the wing displacements for different load cases while in the bottom plots the averaged response for left and right wing is presented.

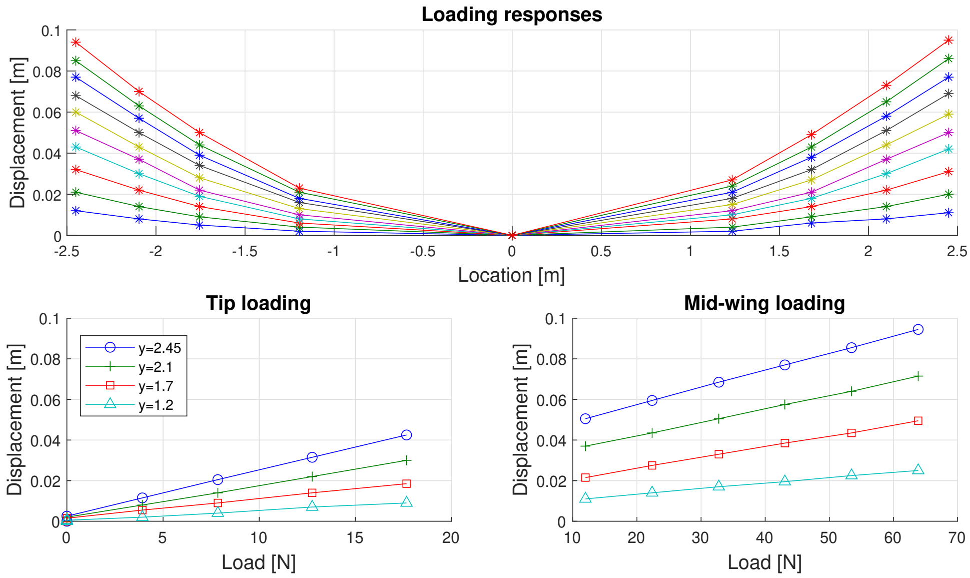

Figure 13: Diana 2 wing displacement responses for varying tip and mid-wing loads.

With all the test results combined FEM model updating was performed using FEMtools software. As the first step, only the wing stiffness parameters were fitted based on the load-displacement results. Then the entire glider model updating was conducted using the individual mass, centre of gravity and GVT results. From the estimated modal analysis, the mode frequencies and the displacement and rotational mode shapes were used for the fitting. Additionally, both of the wings were constrained to have the same structural properties. The updating iterations were then performed until convergence for which the results are presented in Table 4.

Table 4: Updated Diana 2 FEM model comparison to GVT results.

Mode	FEM [Hz]	GVT [Hz]	Diff. [%]	$MAC_{disp}[\%]$	$MAC_{rot}[\%]$
1	7.67	7.57	1.28	98.66	96.15
2	9.86	9.98	-1.14	95.26	92.43
3	14.23	14.18	0.33	97.66	98.66
4	17.28	17.33	-0.27	97.29	98.01
5	20.39	20.09	1.50	81.34	89.74
6	21.18	21.22	-0.21	84.74	74.37
7	23.33	23.50	-0.69	70.09	83.16
8	25.72	26.01	-1.13	91.54	93.32
9	39.61	39.57	0.09	65.20	70.79
10	44.72	45.15	-0.94	77.74	71.17
11	46.92	46.94	-0.03	99.21	95.42
12	53.10	53.11	-0.02	92.50	72.75

As can be seen, the updating procedure reached a solution where the FEM model natural frequencies were within 1.5% of the GVT results while achieving very good matches for most mode shapes. The MAC values were calculated separately for the displacement and rotational mode shapes. This allowed to verify that the updated model is able to capture both motions.

While most modes reached MAC values above 90%, modes 5 to 7 and 9 and 10 remained around $70 - 80\%$. It was observed that while the main motion was captured well, the most noticeable difference was often in one or two nodes being out of phase. The reasons for this could be the modal estimate being sensitive to the selected poles during the estimation process which in turn can be due to higher noise and limited sensitivity of the sensors.

However, a good FEM model should also possess some predictive capabilities. For this purpose, an additional GVT test was conducted on the Diana 2 glider. During this test, lumped masses of 200g were added to both wingtips together with 50g masses that were added to the tips of the horizontal tail. Again, the natural frequencies and the corresponding mode shapes were estimated and compared to the updated FEM model predictions where the same mass modifications were added. These results are presented in Table 5 where the comparison is made with modal parameters obtained with reference accelerometers.

Table 5: Diana 2 FEM model validation with lumped mass modifications.

Mode	FEM [Hz]	GVT [Hz]	Diff. [%]	$MAC_{disp}[\%]$
1	5.50	5.64	-2.47%	98.90
2	7.29	7.82	-6.78%	97.50
3	10.52	10.29	2.31%	96.00
4	11.71	12.82	-8.66%	96.10
5	16.52	16.61	-0.56%	82.60
6	15.74	15.75	-0.08%	90.30
7	18.05	19.19	-5.95%	93.40
8	20.56	21.72	-5.35%	88.50
9	36.83	37.45	-1.66%	42.60
10	39.09	39.98	-2.24%	73.20
11	30.85	32.27	-4.41%	98.10
12	48.12	48.08	0.07%	92.90

As can be seen, in general the FEM model is able to predict the mass modification results quite well. However, there is definitely room for improvement to reduce the difference in frequency for some modes. An option for this would be to also perform a load-displacement test on the tail section and include that to the updating. The mode shapes obtained using reference accelerometers were used for the validation which actually improved the MAC values for many modes as compared to results in Table 4. This was due to the issues with a single node being out of phase not being present in this case. Main outlier being mode 9 which consists of tail side to side movement, 3rd asymmetric wing bending and also in plane 2nd asymmetric bending. While this complex motion is captured well in both the FEM model and GVT results, the in plane bending is out of phase between the two and therefore results in a much lower MAC value.

6 CONCLUSION

In this paper, a ground vibration test of a scaled Diana 2 glider was conducted using the accelerometers, gyroscopes and strain gauges placed across the entire structure. From the vibration test measurements, the modal frequencies were estimated together with displacement, rotational and strain mode shapes. These results were then compared to modal parameters obtained from external reference accelerometers to evaluate the accuracy of the custom data acquisition system built for the Diana 2 glider. The internal sensor results showed good agreement with the reference. Furthermore, it was seen that the addition of gyroscopes to the vibration testing allows to directly measure the rotational mode shapes and reduce the amount of accelerometers required.

A FEM model of the glider was also built and updated using the GVT results. In addition, component mass and centre of gravity measurements together with load-displacement test results were used during the model updating. A good fit was achieved where the FEM model natural frequencies were within 1.5% of the experimental results. Furthermore, both displacement and rotational mode shapes achieved a close match with the test. Finally, the updated FEM model was validated by predicting the effect of lumped mass modifications on the structure and comparing to the corresponding GVT results. The validation results showed a very close match in the mode shapes while the natural frequency prediction showed room for improvement for some modes. However, overall the FEM model fitting results are satisfactory and the model can now be used as part of an aeroelastic model for simulating flexible aircraft flight dynamics with the goal of exploring different approaches for system identification.

ACKNOWLEDGMENTS

The authors would like to thank the Netherlands Aerospace Centre Flight Physics and Loads department (AVFP) for the support and funding of this research project.

7 REFERENCES

[1] Jurisson, A., de Breuker, R., de Visser, C., et al. (2022). Aeroservoelastic flight testing platform development for system identification. AIAA SciTech, AIAA, p. 13. doi:10.2514/6.2022-2169.

[2] Kranjc, T., Slavič, J., and Boltežar, M. (2016). A comparison of strain and classic experimental modal analysis. *Journal of Vibration and Control*, 22, 371–381. ISSN 1077-5463. doi:10.1177/1077546314533137.

[3] Baudismodel.com (2021). Diana 2 (scale 1/3). (accessed: 01.12.2021).

[4] Peeters, B., Van der Auweraer, H., Guillaume, P., et al. (2004). The PolyMAX frequency-domain method: A new standard for modal parameter estimation? *Shock Vib.*, 11(3-4), 395–409.

[5] Allemang, A. J. (2003). The modal assurance criterion (MAC): Twenty years of use and abuse. *Sound Vib*, 14–21.

[6] dos Santos, F. L. M. and Peeters, B. (2016). On the use of strain sensor technologies for strain modal analysis: Case studies in aeronautical applications. *Review of Scientific Instruments*, 87, 102506. ISSN 0034-6748. doi:10.1063/1.4965814.